JAMA Neurology | Original Investigation

Assessing Spinal Cerebrospinal Fluid Leaks in Spontaneous Intracranial Hypotension With a Scoring System Based on Brain Magnetic Resonance Imaging Findings

Tomas Dobrocky, MD; Lorenz Grunder, MD; Philipe S. Breiding, MD; Mattia Branca, MSc; Andreas Limacher, PhD; Pascal J. Mosimann, MD; Pasquale Mordasini, MSc; Felix Zibold, MD; Levin Haeni, MD; Christopher M. Jesse, MD; Christian Fung, MD; Andreas Raabe, MD; Christian T. Ulrich, MD; Jan Gralla, MSc; Jürgen Beck, MD; Eike I. Piechowiak, MD

IMPORTANCE Various signs may be observed on brain magnetic resonance imaging (MRI) in patients with spontaneous intracranial hypotension (SIH). However, the lack of a classification system integrating these findings limits decision making in clinical practice.

OBJECTIVE To develop a probability score based on the most relevant brain MRI findings to assess the likelihood of an underlying spinal cerebrospinal fluid (CSF) leak in patients with SIH.

DESIGN, SETTING, AND PARTICIPANTS This case-control study in consecutive patients investigated for SIH was conducted at a single hospital department from February 2013 to October 2017. Patients with missing brain MRI data were excluded. Three blinded readers retrospectively reviewed the brain MRI scans of patients with SIH and a spinal CSF leak, patients with orthostatic headache without a CSF leak, and healthy control participants, evaluating 9 quantitative and 7 qualitative signs. A predictive diagnostic score based on multivariable backward logistic regression analysis was then derived. Its performance was validated internally in a prospective cohort of patients who had clinical suspicion for SIH.

MAIN OUTCOMES AND MEASURES Likelihood of a spinal CSF leak based on the proposed diagnostic score.

RESULTS A total of 152 participants (101 female [66.4%]; mean [SD] age, 46.1 [14.3] years) were studied. These included 56 with SIH and a spinal CSF leak, 16 with orthostatic headache without a CSF leak, 60 control participants, and 20 patients in the validation cohort. Six imaging findings were included in the final scoring system. Three were weighted as major (2 points each): pachymeningeal enhancement, engorgement of venous sinus, and effacement of the suprasellar cistern of 4.0 mm or less. Three were considered minor (1 point each): subdural fluid collection, effacement of the prepontine cistern of 5.0 mm or less, and mamillopontine distance of 6.5 mm or less. Patients were classified into groups at low, intermediate, or high probability of having a spinal CSF leak, with total scores of 2 points or fewer, 3 to 4 points, and 5 points or more, respectively, on a scale of 9 points. The discriminatory ability of the proposed score could be demonstrated in the validation cohort.

CONCLUSIONS AND RELEVANCE This 3-tier predictive scoring system is based on the 6 most relevant brain MRI findings and allows assessment of the likelihood (low, intermediate, or high) of a positive spinal imaging result in patients with SIH. It may be useful in identifying patients with SIH who are leak positive and in whom further invasive myelographic examinations are warranted before considering targeted therapy.

JAMA Neurol. 2019;76(5):580-587. doi:10.1001/jamaneurol.2018.4921
Published online February 18, 2019.

Supplemental content

Author Affiliations: University Institute of Diagnostic and Interventional Neuroradiology, University of Bern, Inselspital, Bern, Switzerland (Dobrocky, Grunder, Breiding, Mosimann, Mordasini, Zibold, Gralla, Piechowiak); Clinical Trials Unit Bern, Institute of Social and Preventive Medicine, University of Bern, Bern, Switzerland (Branca, Limacher); Department of Neurosurgery, University of Bern, Inselspital, Bern, Switzerland (Haeni, Jesse, Fung, Raabe, Ulrich, Beck); Department of Neurosurgery, Medical Center–University of Freiburg, Freiburg, Germany (Fung, Beck).

Corresponding Author: Tomas Dobrocky, MD, Institute of Diagnostic and Interventional Neuroradiology, University of Bern, Inselspital Bern, Freiburgstrasse 8, Bern CH-3010, Switzerland (tomas.dobrocky@insel.ch).

Spontaneous intracranial hypotension (SIH) is a well-established condition generally presenting with disabling orthostatic headache, occasionally accompanied by other symptoms, such as nausea, vomiting, and neck pain. The first imaging challenge to overcome is to recognize signs of intracranial hypotension on brain magnetic resonance imaging (MRI). The second is to identify an underlying treatable cause, such as a cerebrospinal fluid (CSF) leak. The third is to localize the exact level of the dural breach along the spinal axis.

According to the third edition of the International Classification of Headache Disorders,[1] the criteria required for the diagnosis of headache attributed to low CSF pressure and SIH are (1) low CSF pressure (<60 mm of H_2O) and/or evidence of CSF leakage on imaging; (2) a headache developing in temporal relation to and leading to the discovery of low CSF pressure or CSF leakage; and (3) the absence of a causative mechanism that was better accounted for by another diagnosis in the International Classification of Headache Disorders, third edition.[1] Classic signs of SIH on brain MRI have been reported by Schievink et al[2] and include subdural fluid collections, enhancement of the pachymeninges, engorgement of venous structures, pituitary hyperemia, and sagging of the brain. Other imaging signs have also been reported (**Figure 1**). However, to the best of our knowledge, no validated system integrating these findings to assess the probability of positive spinal imaging demonstrating an underlying spinal CSF leak currently exists. Furthermore, a robust classification system may lead to more standardized diagnostic and therapeutic approaches between headache specialists, including neurologists, neuroradiologists, and neurosurgeons. We aimed to define such a score based on the most reliable brain MRI findings in patients with SIH who have a myelographically and/or surgically confirmed spinal CSF leak.

Key Points

Question Is reliable assessment of a spinal cerebrospinal fluid leak in patients with spontaneous intracranial hypotension possible using a simple predictive score based on brain magnetic resonance imaging findings?

Findings This case-control study involves the development of a simple scoring system integrating 6 relevant brain imaging findings. This 9-point scoring system may help headache specialists objectively assess whether patients with spontaneous intracranial hypotension should further be investigated with invasive tests that use intrathecal contrast media to identify a spinal cerebrospinal fluid leak that might be resolved with an epidural blood patch or microsurgical exploration.

Meaning This appears to be the first brain magnetic resonance imaging–based imaging predictive modeling score to assess the likelihood of a cerebrospinal fluid leak in patients with suspected spontaneous intracranial hypotension that is easily applicable in routine clinical care and could lead to more standardized diagnostic and therapeutic pathways.

Methods

Institutional review board approval was obtained from the Kantonale Ethikkommission Bern for this single-center study. Informed consent was waived owing to the retrospective nature of the study.

Derivation Cohort

Patients With SIH and a Confirmed CSF Leak

Between February 2013 and October 2017, all consecutive patients with SIH who had had a dural CSF leak established on computed tomographic (CT) myelography during evaluation at the study institution were included. Patients usually presented with typical orthostatic headache manifesting within minutes after assuming the upright position and subsided within a few minutes after lying down. The standardized diagnostic workup included detailed clinical history, optic nerve-sheath ultrasonography, lumbar-infusion testing, and a brain MRI followed by dedicated spinal imaging (including native MRI and intrathecal gadolinium-enhanced MRI). On subsequent conventional dynamic myelography, the level of the CSF leak was defined as the area with the earliest epidural contrast spillage. To prevent false-positive findings on postmyelographic CT at the lumbar level, patients were asked to perform a Valsalva maneuver during fluoroscopy. If no leakage was observed on fluoroscopy and postmyelographic CT demonstrated extrathecal contrast confined to the level of the puncture site and the adjacent vertebral level, then it was considered iatrogenic. If no epidural contrast was identified on the first postmyelographic CT, a late-phase postmyelographic CT was performed 4 to 24 hours after initial intrathecal injection to exclude low-flow leaks. In patients with clinical suspicion for SIH, we reevaluated all brain MRIs performed within 4 months before conventional myelography and consecutive postmyelographic CT results.

Brain MRI

At the institution in which this study was conducted, MRI was performed on a 1.5-T or 3-T scanner (Magnetom Avanto and Magnetom Trio; Siemens Medical Solutions). Routine MRI sequences included native and postcontrast sequences (eMethods 1 in the Supplement). In all patients, brain MRI was performed for clinical reasons, but since this was not part of a dedicated study protocol, the acquired sequences were not identical. Patients imaged in external institutions were eligible only if adequate quality and comparable sequences had been performed.

Image Analysis

All MRI studies were assessed independently by 1 board-certified neuroradiologist (T.D.), who had 7 years of experience, and 2 neuroradiology fellows (P.S.B. and L.G.), who each had 2 years of experience. All were blinded to clinical presentation and all other imaging studies performed. Brain MRIs of patients and controls were reviewed on a picture-archiving and communications system station. All relevant sequences were prearranged and stored on an established, fixed, nonmodifiable layout (E.I.P.); a short educational module was provided to each reader before image interpretation. The readers were instructed to assess all signs in each patient and report them in a standardized spreadsheet (eMethods 2 and 3 in the Supplement).

Figure 1. Illustration of Typical Findings on Brain Magnetic Resonance Imaging in Intracranial Hypotension

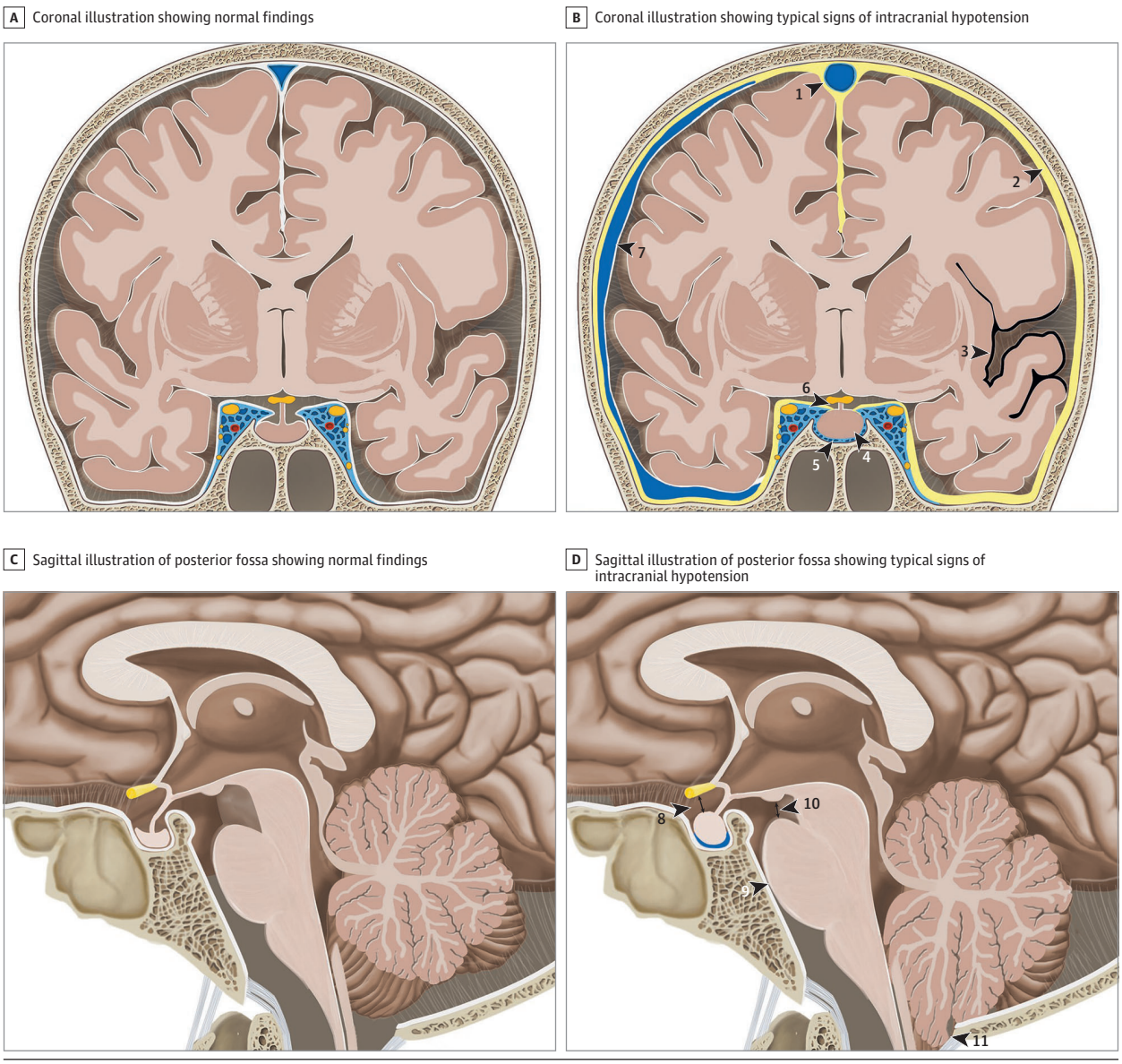

A, Coronal illustration of the brain demonstrating normal findings. B, Coronal illustration of the brain with typical findings in a patient with a spinal cerebrospinal fluid leak with venous engorgement of the superior sagittal sinus (arrowhead 1), pachymeningeal enhancement (arrowhead 2), superficial siderosis (arrowhead 3), enlarged pituitary gland (arrowhead 4), prominent intercavernous sinus (arrowhead 5), effaced suprasellar cistern (arrowhead 6), and subdural fluid collection (arrowhead 7). C, Sagittal illustration of the posterior fossa demonstrating normal findings. D, Sagittal illustration of the posterior fossa with typical findings in patients with a spinal cerebrospinal fluid leak with effaced suprasellar cistern (arrowhead 8; pathologic ≤4 mm), effacement of the prepontine cistern (arrowhead 9; pathologic ≤5 mm), decreased mamillopontine distance (arrowhead 10; pathologic ≤6.5 mm), and low-lying cerebellar tonsils (arrowhead 11).

An updated literature review was performed to identify previously reported signs of intracranial hypotension on brain imaging. We then assessed 7 qualitative items (engorgement of venous sinus, distended inferior intercavernous sinus, pachymeningeal enhancement, midbrain descent [subjective], superficial siderosis, subdural fluid collection [present or absent], and superior surface of the pituitary [concave, flat, or convex]) and 9 quantitative signs (pituitary height, pontomesencephalic angle, suprasellar cistern, prepontine cistern, midbrain descent, venous-hinge angle, mamillopontine angle, tonsillar descent, and area cavum veli interpositi [exact values]) (eTable 1 and eFigures 1 and 2 in the Supplement).

Validation Cohort

The scoring system was subsequently validated in a prospective cohort of 20 consecutive patients who were clinically suspected of having SIH and investigated at the study institution between November 2017 and August 2018. The imaging findings included in the final scoring system were assessed by the same 3 readers (T.D., P.S.B., and L.G.), who were blinded to

clinical presentation and previous imaging studies. The score was calculated and assigned to each patient.

Statistical Analysis

Statistical analysis was performed using Stata version 15 (StataCorp). Descriptive analysis was performed using frequencies and percentages for categorical variables and mean (SD) or median (interquartile range [IQR]) for continuous variables, as well as χ^2 and *t* tests to compare categorical and continuous variables, respectively. The results of all 3 readers were aggregated. Continuous imaging measures were used to calculate a mean between the 3 readers.

Interrater reliability for categorical data was determined by using Fleiss κ. For continuous data, the intraclass correlation coefficient was calculated with the 2-way mixed-effects model estimating absolute agreement. The crude association of each imaging sign with SIH was calculated using mixed-effects logistic regression based on the imaging results of individual readers. Based on descriptive analysis, variables with low agreement among the readers (defined by a κ or intraclass correlation coefficient less than 0.6) were removed from predictive modeling. With the remaining binary variables, we used a predictive model to analyze the significance of the factors using mixed-effects logistic regression. We used multiple imputations to account for missing data, generating 20 data sets based on all other variables. Based on the coefficients of the final model, we built a score and assigned 1 point to variables with a coefficient of 2 or less (minor criteria) and 2 points to variables with a coefficient of more than 2 (major criteria).

The score was calculated for all patients and control participants in the derivation cohort of the study population using the aggregated assessments of the readers. Receiver operating characteristic curve analysis was performed to determine cutoff values for a 3-tier predictive scoring system. (Detailed description of statistical analysis are in eMethods 4 in the Supplement). The score was then internally validated in a cohort of 20 prospectively evaluated patients.

Results

A total of 89 patients were investigated for SIH according to the standard protocol.[3,4] Seventeen patients were excluded owing to missing brain MRI data, imaging older than 4 months prior to diagnosis of the CSF leak, or a recent lumbar puncture (eFigure 3 in the Supplement). Sixteen patients with orthostatic headache with negative multimodal spinal imaging (no extrathecal CSF on dynamic myelography, postmyelography CT, native spine MRI, or gadolinium-enhanced MRI) were not considered for derivation of the score. The final study population therefore consisted of 56 patients with a myelographic CT-confirmed CSF leak, of whom 40 (71%) were female, and 53 (95%) had cases verified intraoperatively. Their mean (SD) age was 44.8 (11. 5) years (range, 18-73 years). The duration of clinical symptoms varied from a few days to several years.

Sixty healthy participants who were matched for age and sex, did not have headaches, and had an unremarkable brain MRI served as control participants. Their mean (SD) age was 46.3 (15.7) years (range, 18-78 years). Of the 60, 42 (70%) were women.

In addition, 11 patients with a myelographically established CSF leak on CT and 9 patients without a CSF leak were included in the validation cohort. Their mean (SD) age was 44.3 years (15.0) years (range, 15-64 years), with an equal sex distribution.

Many patients were previously included in 3 other articles[3-6] investigating different outcome measures, including optic nerve-sheath ultrasonography, surgical dural closure, and CSF dynamics. Despite this study population overlap, none of the previous articles reported on brain MRI findings.

Qualitative and Quantitative Signs

The presence of all qualitative signs ascertained by subjective assessment was more prevalent in patients with SIH and a CSF leak than control participants (subdural fluid collection: 30 of 56 patients with SIH [54%] vs 1 of 60 control participants [2%]; $P < .001$; pachymeningeal enhancement: 43 patients with SIH [83%]; 1 control participant [2%]; $P < .001$; engorgement of venous sinus: 37 patients with SIH [66%]; 0 control participants; $P < .001$; distended inferior intercavernous sinus: 25 patients with SIH [47%]; 0 control participants; $P < .001$; superficial siderosis: 5 patients with SIH [12%]; 0 control participants; $P < .001$; and midbrain descent: 15 patients with SIH [27%]; 4 control participants [7%]; $P = .005$). All 3 shapes of the superior border of the pituitary gland were reported in both groups, the convex shape being the most common in patients with SIH and confirmed CSF leak (concave: 4 of 56 patients with SIH [7%]; 25 of 60 control participants [42%]; $P = .04$; flat: 17 of 56 patients with SIH [30%]; 30 of 60 control participants [50%]; $P < .001$; convex: 35 of 56 patients with SIH [63%]; 5 of 60 control participants [8%]; $P < .001$), with fair degree of interreader agreement (κ = 0.346). The difference in mean values of all continuous variables between patients with SIH and control participants, as well as interobserver agreement for all qualitative and quantitative values, are shown in **Table 1**.

Predictive Score

The crude and adjusted associations are provided in eTable 2 in the Suppplement. For continuous variables, the area under the curve and the optimal cutoff point with corresponding sensitivity and specificity were calculated and are presented in eTable 3 in the Supplement. Based on descriptive analysis, variables with low agreement between the readers (κ or intraclass correlation coefficient less than 0.60) were removed from predictive modeling: midbrain descent distance, midbrain descent (a subjective variable), tonsillar descent, upper contour of the pituitary gland, venous-hinge angle, intercavernous sinus, and pontomesencephalic angle. We performed a backward selection that excluded siderosis from the predictive model. Furthermore, the area of the cistern of vellum interpositum was removed owing to complex measurement, and the pituitary height was removed given the physiological range according to age and sex.

In total, 6 imaging findings were included in the final scoring system. Three criteria were considered major

Table 1. Demographic Data and Imaging Signs in Patients With Spontaneous Intracranial Hypotension and Control Participants

Sign	Participants, No. (%)		*P* Value	Interobserver Agreement[a]
	Spontaneous Intracranial Hypotension (n = 56)	Control (n = 60)		
Age, mean (SD), y	44.8 (11.5)	46.3 (15.7)	.58	NA
Female	40 (71)	42 (70)	.87	NA
Engorgement of venous sinus	37 (66)	0	<.001	0.684
Distended inferior intercavernous sinus	25 (47)	0	<.001	0.536
Pachymeningeal enhancement	43 (83)	1 (2)	<.001	0.803
Midbrain descent[b]	15 (27)	4 (7)	.005	0.436
Superficial siderosis	5 (12)	0	.01	1.000
Subdural fluid collection	30 (54)	1 (2)	<.001	0.859
Superior surface of pituitary				
Concave	4 (7)	25 (42)	.04	0.346
Flat	17 (30)	30 (50)	<.001	
Convex	35 (63)	5 (8)	<.001	
Angle measurements, mean (SD), degrees				
Venous-hinge	95.4 (15.4)	95.8 (13.7)	.87	0.509
Pontomesencephalic	48.9 (10.5)	60.4 (7.3)	<.001	0.581
Size measurements, mean (SD), mm				
Pituitary height	7.6 (1.4)	4.9 (1.5)	<.001	0.754
Difference of pituitary height to age-adjusted and sex-adjusted reference	2.3 (1.3)	−0.4 (1.3)	<.001	0.740
Suprasellar cistern	3.1 (1.9)	6.5 (1.9)	<.001	0.899
Prepontine cistern	4.1 (1.5)	6.1 (1.5)	<.001	0.654
Midbrain descent[c]	2.3 (2.7)	2.8 (2.3)	.28	−0.058
Mamillopontine distance	5.7 (1.7)	7.5 (1.1)	<.001	0.867
Tonsillar descent	5.5 (2.5)	7.1 (2.7)	.002	−0.033
Area cavum veli interpositi, mean (SD), mm^2	37.7 (27.1)	58.2 (24.6)	<.001	0.795

Abbreviation: NA, not applicable.

[a] For interobserver reliability, coefficients were calculated for each reader pair (reader 1 vs reader 2, reader 1 vs reader 3, and reader 2 vs reader 3), and then a mean was calculated to obtain the overall interobserver agreement, expressed by the κ value for qualitative signs and the interclass correlation coefficient for quantitative signs. For tonsillar herniation, the distance between foramen magnum (McRae line) and the tip of the cerebellar tonsil was measured on parasagittal images.

[b] Subjective appraisal.

[c] Iter to incisural line.

Table 2. Six Imaging Signs With Good Discriminative Power and Interrater Agreement That Were Included in the Final Diagnostic Score and Assigned Score Points

Characteristic	Coefficient (95% CI)	Odds Ratio (95% CI)	*P* Value	Score Points
Engorgement venous sinus	2.95 (1.18-4.72)	19.12 (3.26-112.30)	.001	2
Pachymeningeal enhancement	4.04 (2.50-5.59)	57.01 (12.18-266.78)	<.001	2
Subdural fluid collection	1.54 (−0.10 to 3.17)	4.65 (0.90-23.92)	.07	1
Suprasellar cistern[a]	3.48 (2.36-4.60)	32.32 (10.55-99.02)	<.001	2
Prepontine cistern[b]	1.47 (0.41-2.52)	4.34 (1.51-12.47)	.007	1
Mamillopontine distance[c]	1.13 (0.07-2.19)	3.08 (1.07-8.90)	.04	1

[a] ≤4 mm.

[b] ≤5 mm.

[c] ≤6.5 mm.

(2 points each): pachymeningeal enhancement, engorgement of venous sinus, and effacement of the suprasellar cistern of 4.0 mm or less. The other 3 were considered minor (1 point each): subdural fluid collection, effacement of the prepontine cistern of 5.0 mm or less, and mamillopontine distance of 6.5 mm or less (**Table 2**). An illustrative case showing these imaging findings is provided in **Figure 2**. The diagnostic scale ranges from 0 (minimum) to a score of 9 (maximum).

Based on the chosen cutoff values in the receiver operating characteristic analysis, participants were further classified into 3 groups corresponding to the probability of finding a spinal CSF leak: low (≤2), intermediate (3-4), and high (≥5). The diagnostic performance of the score in the derivation cohort was compared with the initial clinical diagnosis (**Figure 3**). In total, 60 patients were classified as having a low probability of a spinal CSF leak (score ≤2). This group included 56 true-negative and 4 false-negative assessments, resulting in a 92.9% sensitivity and 93.3% specificity for this cutoff value. At the other end of the spectrum, 45 patients were classified as having a high probability of a spinal CSF leak (score ≥5). In all but 1 patient, a spinal CSF leak had been correctly identified (ie, 44 true-positive and 1 false-positive assessments, respectively), providing a 78.6% sensitivity and 98.3% specificity for this cutoff value (eTable 4 and 5 in the Supplement).

There was no significant difference in age and sex between the derivation and validation cohort. In the valida-

Figure 2. Imaging Findings Included in the Final Diagnostic Score

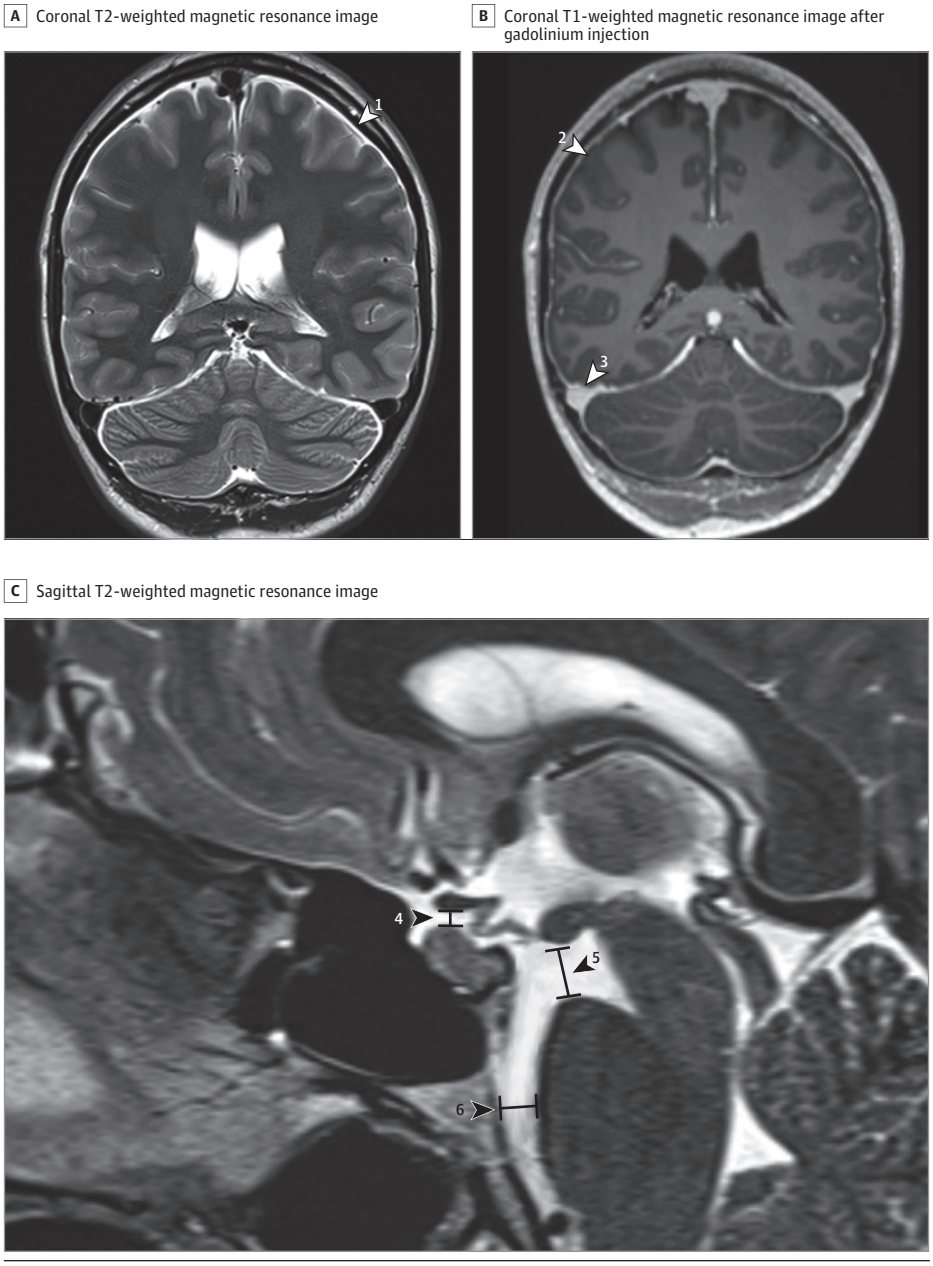

A, Coronal T2-weighted magnetic resonance imaging (MRI) with subdural effusion (white arrowhead 1). B, Coronal T1-weighted MRI after gadolinium injection of the same patient, with dural enhancement (white arrowhead 2) and venous engorgement (white arrowhead 3). C, Sagittal T2-weighted MRI with effaced suprasellar cistern (black arrowhead 4; pathologic ≤4 mm), decreased mamillopontine distance (black arrowhead 5; pathologic ≤6.5 mm), and effaced prepontine cistern (black arrowhead 6; pathologic ≤5 mm).

tion cohort, 7 patients with true-negative results were correctly classified as having a low probability of a spinal CSF leak (score ≤2), providing a 100% sensitivity and 77.8% specificity for this cutoff value (eTable 5 and 6 in the Supplement). Nine of 10 patients with a high probability of a spinal CSF leak (score ≥5) were correctly identified (ie, 9 true-positive results and 1 false-positive result), providing a 81.8% sensitivity and 88.9% specificity for this cutoff value. The area under the receiver operating characteristic curve for the final score was 0. 98 (95% CI, 0.97-0.99) for the derivation cohort and 0.93 (95% CI, 0.79-1.00) for the validation cohort (eFigure 4 in the Supplement).

Discussion

The scoring system we propose integrates the 6 most relevant brain MRI findings and allows stratification of patients with SIH according to the presence of extradural contrast on postmyelographic CT. The score is based on 3 qualitative and 3 quantitative signs and provides high diagnostic accuracy. The score is intended to guide patient management and facilitate communication between specialists. We believe that this may serve to better standardize the diagnostic and therapeutic pathways of these patients. Indeed, currently, a dynamic myelo-

Figure 3. Predictive Model Scores

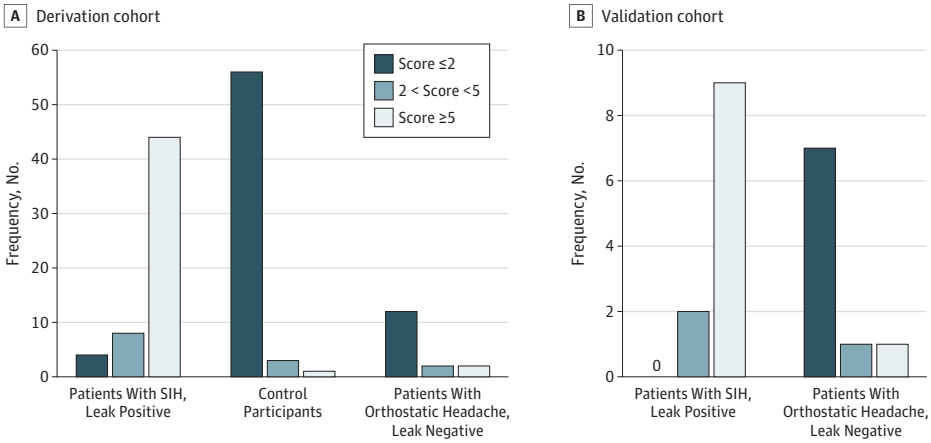

A, Scores for individuals in the derivation cohort: patients with spontaneous intracranial hypotension (SIH) who are leak positive, healthy control participants, and patients with orthostatic headache without a cerebrospinal fluid leak. B, Scores for individuals in the internal validation cohort including patients with spontaneous intracranial hypotension and a myelographically confirmed leak and patients presenting with orthostatic headache without a cerebrospinal fluid leak.

graphic technique is required to localize a CSF leak precisely.[7] Such invasive explorations, however, are time consuming, costly, and demanding for the patients and caregivers. Ideally, they should be reserved for those who have a high likelihood of a positive finding. Selection based solely on clinical findings lacks objectivity, often leads to imprudent invasive examinations, and may expose the patient to complications. Since brain MRI is the first imaging of choice in the workup of patients with clinical suspicion for SIH, to rule out an underlying intracranial pathology, the proposed scoring system allows disambiguation of which candidates may benefit from further spinal imaging or more invasive methods.

We suggest classifying patients in 3 groups according to specific cutoff scores: those with a score of 5 or more have a very high probability of a spinal CSF leak and therefore a high likelihood of a positive result on dynamic conventional or CT myelography. In these patients, an epidural blood patch should be promptly considered. Preventing delay in diagnosis is important since prolonged dysregulation of the CSF system may entail rebound intracranial hypertension after closure of the dural tear.[8] In patients with a low likelihood of a CSF leak (a score ≤2), noninvasive spine imaging is recommended to exclude the presence of epidural CSF. However, the probability of a CSF leak in these patients is very low, and thus invasive diagnostic examinations requiring intrathecal application of contrast and ionizing radiation are not advocated. Patients with an intermediate probability of a spinal CSF leak (scores 3-4) require a case-by-case discussion and may benefit from additional adjunctive explorations, such as a lumbar infusion test[5] or transorbital ultrasound of the optic nerve-sheath[3] before more invasive diagnostic examinations are initiated.

Pathophysiologically speaking, the Monro-Kellie hypothesis states that volume loss in 1 compartment within a closed and well-regulated system must be compensated by a volume increase in other compartments. The depletion of CSF in the subarachnoid space should therefore first lead to a compensatory volume increase in the venous system, the most compliant compartment, followed by increased volume in the subdural space. These compensatory mechanisms may thus explain the typical brain imaging findings of patients with SIH, particularly venous engorgement with pachymeningeal enhancement, pituitary hyperemia, and/or subdural fluid collections.[6] The major issue with patients expressing typical signs of SIH on brain MRI is that none of these signs is pathognomonic. As reported by Kranz et al,[9] pachymeningeal enhancement in SIH tends to be smooth and diffuse. However, thickened pachymeningeal enhancement may also be observed after lumbar puncture; craniotomy; and infectious, inflammatory, or tumor-cell spread (meningeal carcinomatosis) to the meninges. Moreover, pituitary gland enlargement is an unreliable sign of SIH, given the physiological variation according to age and sex or the possibility of an underlying infiltrative process, such as hypophysitis or adenoma. It is not uncommon for patients with SIH to present with an unremarkable brain MRI; some authors report this in up to 20% of patients.[2] Nonetheless, as shown in the largest study[7] published so far, to our knowledge (of 99 participants, of whom 54 of which had an established leak on CT myelography), dural enhancement, venous engorgement, and midbrain descent was present in 83%, 75%, and 62% of patients, respectively.

In this study, no patient of the derivation or validation cohort with an established spinal CSF leak had a normal brain MRI (with scores of 0 and 1). Only 4 of 56 participants (7.1%) in the derivation cohort and none in the validation cohort had a score of 2. As is often seen in patients, calcified discogenic microspurs or dural dehiscence at the axilla of a nerve-root sleeve are now well-established underlying causes of a CSF leak.[4] Despite our best efforts and thorough contrast-enhanced myelographic explorations, we were unable to demonstrate a single case of so-called CSF-venous fistula in this study, which remains a controversial causative mechanism in patients with SIH without an established CSF leak.

As reported by Capizazano et al,[10] patients with a long-standing history of SIH are more likely to display atypical clinical and imaging findings, which was also observed in this study. This may be because of compensatory mechanisms in long-standing states that may render the usual findings less conspicuous. Another factor potentially affecting brain imaging may be the dynamics of the leak (ie, low flow vs high flow).

Finally, patients with orthostatic headache without confirmation of CSF leakage despite exhaustive multimodal examination pose a real diagnostic challenge, and so far the underlying pathomechanism is not well understood. These results show that most patients in this subgroup present with a low score (Figure 3). However, there are few individuals with an intermediate and high score. We can only speculate if these are the false-negative results on multimodal imaging, or if other pathological mechanisms such as hypercompliance of the thecal sac, CSF hyperresorption, stenosis of the inferior vena cava,[11] or CSF-venous fistula may provide the explanation.

The major strength of this study is the large number of consecutively enrolled patients with SIH evaluated in a multimodal diagnostic approach including optic nerve-sheath ultrasound, lumbar infusion test, and brain MRI, followed by dedicated spinal imaging including native MRI, gadolinium-enhanced MRI, and CT myelography. Second, comparison of patients with SIH who are leak-positive with a CT myelography–established CSF leak with healthy matched control participants. Third, blinded imaging analysis performed independently by 3 neuroradiologists. Finally, the good discriminatory ability of the proposed score was confirmed in a real-life setting in a matched validation cohort.

Limitations

The main limitations of this study are its retrospective and monocentric characteristics. Moreover, the image readers may have been biased to report more positive signs once 1 had been identified, considering the list of qualitative parameters they were provided with. Finally, other causes of SIH, such as CSF-venous fistulas, may be more prevalent than the data suggest in patients without an established myelographic leak. This raises questions about the generalizability of the proposed scoring system, which still requires external and prospective validation in a broader population.

Conclusions

The relatively simple and easy-to-use scoring system we propose integrates the 6 most reliable brain MRI findings observed in patients with SIH and a CSF leak. The likelihood to exclude or identify an underlying spinal CSF leak (with high, intermediate, or low probability) may be useful to triage patients who may benefit from more invasive myelographic examinations and subsequent targeted therapy.

ARTICLE INFORMATION

Accepted for Publication: December 20, 2018.

Published Online: February 18, 2019. doi:10.1001/jamaneurol.2018.4921

Author Contributions: Dr Dobrocky had full access to all of the data in the study and takes responsibility for the integrity of the data and the accuracy of the data analysis. Drs Beck and Piechowiak contributed equally as co–last authors.
Concept and design: Dobrocky, Grunder, Branca, Limacher, Mordasini, Raabe, Ulrich, Gralla, Beck, Piechowiak.
Acquisition, analysis, or interpretation of data: Dobrocky, Grunder, Breiding, Branca, Limacher, Mosimann, Mordasini, Zibold, Haeni, Fung, Gralla, Beck, Piechowiak.
Drafting of the manuscript: Dobrocky, Branca, Mosimann, Mordasini, Zibold.
Critical revision of the manuscript for important intellectual content: Dobrocky, Grunder, Breiding, Branca, Limacher, Mosimann, Mordasini, Zibold, Haeni, Fung, Raabe, Ulrich, Gralla, Beck, Piechowiak.
Statistical analysis: Branca, Limacher, Mordasini.
Administrative, technical, or material support: Dobrocky, Grunder, Mordasini, Fung, Ulrich, Gralla, Piechowiak.
Supervision: Dobrocky, Limacher, Mosimann, Mordasini, Raabe, Beck, Piechowiak.

Conflict of Interest Disclosures: Dr Mossiman receives Swiss National Science Foundation grants for research on brain aneurysms. Dr Gralla reports acting as a global principal investigator of Solitaire FR Thrombectomy for Acute Revascularization study; a clinical events committee member of the Prospective, Multicenter, Observational, Single-Arm European Registry on the ACE Reperfusion Catheters and the Penumbra System in the Treatment of Acute Ischemic Stroke (PROMISE) study (Penumbra); and the principal investigator for the Solitaire with the Intention for Thrombectomy (SWIFT DIRECT) study (Medtronic). Dr Gralla also reports serving as a consultant for Medtronic and receiving Swiss National Science Foundation grants for magnetic resonance imaging in stroke. Dr Beck reports acting as a global principal investigator of Swiss Trial of Decompressive Craniectomy versus Best Medical Treatment of Spontaneous Supratentorial Intracerebral Hemorrhage (SWITCH) and To Scan or Not to Scan (TOSCAN) studies and has receiving a Swiss National Science Foundation grant for ultrasound perfusion imaging. No other disclosures were reported.

Data Availability Statement: The datasets analyzed during the current study are not publicly available owing to preclusion from dissemination under Swiss federal law regulations. However, they are available from the corresponding author on reasonable request. Where not in conflict with constraints of the original ethical approval under which the data were collected, pseudoanonymized data will be made available for appropriate collaborative research, subject to appropriate ethical approval being gained for such use.

Additional Contributions: We thank Anja Giger, Department of Neurosurgery, University of Bern, Inselspital, for the provided illustrations. She was not compensated for her contributions.

REFERENCES

1. Vincent M, Wang S; Headache Classification Committee of the International Headache Society. The international classification of headache disorders, 3rd edition. *Cephalalgia*. 2018;38(1):1-211. doi:10.1177/0333102417738202

2. Schievink WI. Spontaneous spinal cerebrospinal fluid leaks and ongoing investigations in this area. *JAMA*. 2006;295(19):2286-2296. doi:10.1001/jama.295.19.2286

3. Fichtner J, Ulrich CT, Fung C, et al. Management of spontaneous intracranial hypotension—transorbital ultrasound as discriminator. *J Neurol Neurosurg Psychiatry*. 2016;87(6):650-655. doi:10.1136/jnnp-2015-310853

4. Beck J, Ulrich CT, Fung C, et al. Diskogenic microspurs as a major cause of intractable spontaneous intracranial hypotension. *Neurology*. 2016;87(12):1220-1226. doi:10.1212/WNL.0000000000003122

5. Beck J, Fung C, Ulrich CT, et al. Cerebrospinal fluid outflow resistance as a diagnostic marker of spontaneous cerebrospinal fluid leakage. *J Neurosurg Spine*. 2017;27(2):227-234. doi:10.3171/2017.1.SPINE16548

6. Beck J, Gralla J, Fung C, et al. Spinal cerebrospinal fluid leak as the cause of chronic subdural hematomas in nongeriatric patients. *J Neurosurg*. 2014;121(6):1380-1387. doi:10.3171/2014.6.JNS14550

7. Kranz PG, Luetmer PH, Diehn FE, Amrhein TJ, Tanpitukpongse TP, Gray L. Myelographic techniques for the detection of spinal CSF leaks in spontaneous intracranial hypotension. *AJR Am J Roentgenol*. 2016;206(1):8-19. doi:10.2214/AJR.15.14884

8. Kranz PG, Amrhein TJ, Gray L. Rebound intracranial hypertension: a complication of epidural blood patching for intracranial hypotension. *AJNR Am J Neuroradiol*. 2014;35(6):1237-1240. doi:10.3174/ajnr.A3841

9. Kranz PG, Gray L, Amrhein TJ. Spontaneous intracranial hypotension: 10 myths and misperceptions. *Headache*. 2018;58(7):948-959. doi:10.1111/head.13328

10. Capizzano AA, Lai L, Kim J, et al. Atypical presentations of intracranial hypotension: comparison with classic spontaneous intracranial hypotension. *AJNR Am J Neuroradiol*. 2016;37(7):1256-1261. doi:10.3174/ajnr.A4706

11. Kumar N, Neidert NB, Diehn FE, Campeau NG, Morris JM, Bjarnason H. A novel etiology for craniospinal hypovolemia: a case of inferior vena cava obstruction. *J Neurosurg Spine*. 2018;29(4):452-455. doi:10.3171/2018.2.SPINE171373